Class I TCP transcription factors regulate trichome branching and cuticle development in Arabidopsis

Alejandra Camoirano, Agustín L. Arce, Federico D. Ariel, Antonela L. Alem, Daniel H. Gonzalez and Ivana L. Viola*

Instituto de Agrobiotecnología del Litoral (CONICET-UNL), Cátedra de Biología Celular y Molecular, Facultad de Bioquímica y Ciencias Biológicas, Universidad Nacional del Litoral, 3000 Santa Fe, Argentina

***Correspondence:**
Ivana L. Viola, Instituto de Agrobiotecnología del Litoral (CONICET-UNL), Centro Científico Tecnológico CONICET Santa Fe, Colectora Ruta Nac. Nº 168 km 0, Paraje el Pozo s/n, 3000 Santa Fe, Argentina. Phone: +54-342-4511370 (5021)
E-mail: iviola@fbcb.unl.edu.ar

Author e-mails: Alejandra Camoirano: camoiranoa@gmail.com; Agustín L. Arce: aarce@fbcb.unl.edu.ar; Federico D. Ariel: fariel@fbcb.unl.edu.ar; Antonela L. Alem: antoalem.aa@gmail.com; Daniel Gonzalez: dhgonza@fbcb.unl.edu.ar; Ivana L. Viola: iviola@fbcb.unl.edu.ar

Highlight: Class I TCP transcriptional regulators directly modulate the expression of MYB and SHINE transcription factors to control trichome branch number and cuticle development in *Arabidopsis*.

ABSTRACT

Trichomes and the cuticle are two specialized structures of the aerial epidermis important for plant organ development and interaction with the environment. In this study, we report that plants affected in the function of the class I TEOSINTE BRANCHED 1, CYCLOIDEA, PCF (TCP) transcription factors TCP14 and TCP15 from *Arabidopsis thaliana* show overbranched trichomes in leaves and stems and increased cuticle permeability. We found that TCP15 regulates the expression of MYB106, a MIXTA-like transcription factor involved in epidermal cell and cuticle development, and overexpression of MYB106 in a *tcp14 tcp15* mutant reduces trichome branch number. TCP14 and TCP15 are also required for the expression of the cuticle biosynthesis genes *CYP86A4*, *GPAT6* and *CUS2*, and of *SHN1* and *SHN2*, two AP2/EREBP transcription factors required for cutin and wax biosynthesis. *SHN1* and *CUS2* are also targets of TCP15, indicating that class I TCPs influence cuticle formation acting at different levels, through the regulation of MIXTA-like and SHN transcription factors and of cuticle biosynthesis genes. Our study indicates that class I TCPs are coordinators of the regulatory network involved in trichome and cuticle development.

KEYWORDS: cuticle, trichome, TCP transcription factors, MIXTA-like transcription factors, SHN, *Arabidopsis thaliana*.

INTRODUCTION

The epidermis is the outermost layer of plant cells and constitutes a protective tissue that forms an interface between the plant and its environment. Besides pavement cells, the epidermal tissue contains several morphologically distinct cell types including guard cells and trichomes. Trichomes are large specialized cells from the epidermis distributed on aerial parts that play a key role in development and help to protect the plant from excess transpiration, high temperature, radiation, ultraviolet light, and herbivore attack (Mauricio and Rausher, 1997; Wagner *et al.*, 2004; Serna and Martin, 2006). In *Arabidopsis thaliana*, trichomes are single living cells found in rosette leaves, stems, cauline leaves, and sepals, but not in hypocotyls or cotyledons. Trichome morphology and density varies in different organs. In rosette leaves, mature trichomes are polarized cells with three branches and a large nucleus located at the lower branch point (Hülskamp et al., 1994), whereas cauline leaf and stem trichomes are less branched and unbranched, respectively (Telfer *et al.*, 1997). During trichome development, after cell fate determination, progenitor cells stop division and switch to endoreplication, followed by enlargement and protrusion from the epidermal layer (Mathur, 2006). Branching is influenced, among other factors, by the ploidy of trichome cells. In *Arabidopsis* rosette leaves, two branching events give trichomes their characteristic three-branch morphology (Mathur, 2006). The genetic network regulating trichome spacing and differentiation has been extensively studied and several genes that are required for trichome development have been identified (Tian *et al.*, 2017; Xiao *et al.*, 2017). More than 15 genes were shown to function as activators or suppressors of branch initiation. Among these, some genes influence branching directly, while others control branch number in an endoreplication-dependent manner (reviewed by Schellmann and Hülskamp, 2005).

In aerial organs, the epidermis is covered with a hydrophobic layer, the cuticle, which functions as a diffusion barrier providing protection against desiccation and external environmental stresses and preventing organ fusion. The plant cuticle is composed of cutin, an insoluble polyester of primarily long-chain hydroxy fatty acids which is synthesized on the surface of the outer epidermal cell wall, and a variety of organic solvent-soluble lipids that are collectively termed waxes (Samuels *et al.*, 2008). The biosynthetic pathways of the waxes and cutin are well described (Yeats and Rose, 2013). Cutin monomers are synthesized in the endoplasmic reticulum by the modification of plastid derived C_{16} and C_{18} fatty acids yielding variously oxygenated fatty acid-glycerol esters. This process involves acyl-activating enzymes of the LONG-CHAIN ACYL-COA SYNTHETASE (LACS) family, cytochrome

P450 enzymes of the CYP86A and CYP77A families, and glycerol-3-phosphate acyltransferases of the GLYCEROL-3-PHOSPHATE SN-2-ACYLTRANSFERASE (GPAT) family (Pollard *et al*., 2008). Wax monomers are mainly very long-chain fatty acids (VLCFA) generated from C_{16} acyl-CoA by the fatty acid elongase (FAE) complex (Yeats and Rose, 2013). These compounds are then transformed by a series of ECERIFERUM (CER) enzymes, such as CER1, CER2, CER3 and CER4 (Javelle et al., 2011), to primary and secondary alcohols, alkanes, ketones, and wax esters (Pollard *et al.*, 2008; Samuels *et al.*, 2008; Li-beisson *et al.*, 2013). After the synthesis, wax and cutin precursors are exported from the endoplasmic reticulum across the plasma membrane to the nascent cuticular membrane by poorly understood mechanisms (Yeats and Rose, 2013). The regulatory steps of cuticle formation are poorly understood. WAX INDUCER1/SHINE1 (WIN1/SHN1) was the first transcription factor identified as having a role in cuticle biosynthesis. SHN1 is part of a clade of the AP2/EREBP transcription factor family from *Arabidopsis* with three members (SHN1-3) that induce the expression of genes encoding enzymes of the cutin and wax biosynthesis pathways (Aharoni *et al*., 2004). MYB transcription factors are also involved in the regulation of wax and cutin biosynthesis. MYB96 and MYB30 regulate wax production in response to stress (Raffaele et al., 2008; Seo et al., 2011) and MYB41 negatively regulates cutin accumulation (Cominelli et al., 2008). More recently, two related MYB transcription factors, MYB106/NOK and MYB16, were identified as regulators of cuticle biosynthesis genes (Oshima *et al*., 2013; Oshima and Mitsuda, 2013). It has been proposed that these proteins directly activate the expression of *SHN1* and some cuticle biosynthesis genes (Oshima *et al*., 2013). MYB106 and MYB16 belong to the subgroup 9 of R2R3 MYB transcription factors along with snapdragon MIXTA and are so defined as MIXTA-like transcription factors (Stracke *et al*., 2001). In addition to this, *Arabidopsis* plants with reduced MYB106 and/or MYB16 function exhibit overbranched trichomes, indicating that they act as negative regulators of trichome branch formation (Folkers *et al*., 1997; Jakoby *et al*., 2008; Oshima *et al*., 2013).

TEOSINTE-BRANCHED1/CYCLOIDEA/PCF (TCP) proteins constitute a family of plant-specific transcription factors that play important roles during plant growth and development (Martín-Trillo and Cubas, 2010; Uberti Manassero *et al*., 2013; Nicolas and Cubas, 2016). TCP proteins (TCPs) have a conserved domain involved in DNA binding and dimerization. Based on distinctive features present both within and outside this domain, TCPs are divided into classes I and II (Cubas *et al*., 1999). Class I proteins participate in the regulation of growth patterns through the control of cell proliferation and hormone signaling pathways

(Danisman, 2016; Nicolas and Cubas, 2016). Two members of the class I, TCP14 and TCP15 from *Arabidopsis*, were shown to be redundant in the control of internode elongation (Kieffer *et al.*, 2011), leaf and flower development (Uberti-Manassero *et al.*, 2012; Lucero *et al.*, 2015; 2017), immunity (Li *et al.*, 2018), and hypocotyl elongation during the response to high temperature (Ferrero *et al.*, 2019). Due to this redundancy, studies with dominant repressor forms of TCP14 and TCP15 were also performed. These studies reported that plants expressing such repressive forms show overbranched trichomes in rosette leaves (Kieffer *et al.*, 2011; Li *et al.*, 2012). For TCP15, this is associated with increased endoreplication in trichomes and cotyledons (Li *et al.*, 2012). These results suggest that TCP14 and/or TCP15 may be involved in regulating trichome branch number. However, experiments with dominant repressor forms do not rule out that other, redundant class I TCPs are indeed involved. In this study, by using loss-of-function mutants, we show that TCP14 and TCP15 actually participate in the specialization of the aerial epidermis controlling trichome branching and also cuticle development. Our results indicate that these TCPs exert these functions by controlling the expression of the *MYB106* and *SHN1* transcription factor genes and of cuticle biosynthesis genes. These results provide novel insights into the development of epidermal tissues and describe a functional relationship between TCP, MIXTA-like and SHN transcription factors during this process.

MATERIALS AND METHODS

Plant material and growth conditions

All the experiments were performed on Arabidopsis (*Arabidopsis thaliana*) accession Col-0. Mutant lines *tcp14-6*, *tcp15-3* and *tcp14-4 tcp15-3* (Kieffer *et al.*, 2011), the *myb106-2* mutant (CS911632), lines expressing *pMYB106::GUS* and *pMYB16::GUS* (Oshima *et al.*, 2013), *35S::TCP15-RFP* (Viola *et al.*, 2016), *35S::TCP15-GFP* (Ferrero *et al.*, 2019) and plants that express TCP15-EAR from the *TCP15* promoter (Uberti-Manassero *et al.*, 2012) were previously described. *tcp15-3 myb106-2*, *35S::TCP15-RFP myb106-2*, *35S::TCP15-RFP pMYB16::GUS* and *35S::TCP15-RFP pMYB106::GUS* lines were generated by crossing. Plants were grown on soil or in plates containing 0.5X Murashige and Skoog (MS) medium and 0.8% agar at 23°C under long-day conditions (16 h light/8 h dark) at a light intensity of 100 µmol m^{-2} s^{-1}. All seeds were surface-sterilized and cold-treated at 4°C for 4 days in the dark to synchronize germination.

DNA constructs and plant transformation

To express *MYB106* from the *35SCaMV* promoter, a pENTR/D-TOPO clone harboring the complete coding sequence of *MYB106* (TOPO-U18-G02), obtained from the Arabidopsis Biological Resource Center (ABRC, Ohio State University), was used for LR recombination into the binary vector pFK-210 (Hellens *et al.*, 2000). The construct was introduced into *Agrobacterium tumefaciens* LB4404. *Arabidopsis* transgenic lines were generated by the *Agrobacterium*-mediated floral dip transformation method (Clough and Bent, 1999). Transformed plants grown on soil were selected on the basis of BASTA resistance and RNA expression levels were measured by RT-qPCR. The primers used for PCR amplifications are listed in Supplementary Table S1.

Phenotypic analysis

To analyze leaf trichome morphology, the fully expanded first two leaves were used. For stem trichome morphology, fully grown stems were cut at the base, the first 2 cm were removed, and the following 1.5 cm was collected. All samples were collected in FAA (formalin-acetyl alcohol-acetic anhydride-water, 10:50:5:35 v/v), incubated for 3 to 4 hours, and then cleared in 70% ethanol. Trichome branch number was analyzed under a LEICA Stereo Microscope (MZ10F) and photographed with a LEICA DFC7000 T camera. At least 8 plants per genotype were analyzed in each experiment.

RNA isolation and analysis

RNA extractions were performed using Trizol reagent (Invitrogen) followed by LiCl precipitation. Quantification of transcript levels was carried out by RT-qPCR. The cDNA was obtained by reverse transcription using 1.5-2.0 µg of RNA with oligodTv primer and MMLV reverse transcriptase (Promega). The qPCR reactions were performed in StepOne™ Real Time PCR System or StepOnePlus™ Real Time PCR System thermocyclers (LifeTechnologies™). The reactions were carried out in a final volume of 20 µL with reaction buffer provided by the manufacturer (10x), 3 mM $MgCl_2$, 0.15 U of *Taq* Pegasus DNA polymerase (PBL, Argentina), 62.5 µM dNTPs, 1 µL SYBR Green, 0.4 µL of specific oligonucleotides (the concentration was optimized for each pair of primers) and 10 µL of a cDNA dilution. A comparative C_t method was used to calculate relative transcript levels, with *ACT2* and *ACT8* actin genes as normalizers (Charrier *et al.*, 2002). Primers used for RT-qPCR are listed in Supplementary Table S1.

β-Glucuronidase assay

β-Glucuronidase (GUS) activity was analyzed by histochemical staining using the chromogenic substrate 5-bromo-4-chloro-3-indolyl-β-D-glucuronic acid (X-gluc) as described by Vitha (2012). Whole seedlings were immersed in a 0.5 µg/µL X-gluc solution in 50 mM citrate-HCl buffer, pH 7.0, and 0.05% Triton X-100. Vacuum was applied for 5 min and reactions were incubated in darkness at 37°C during 16 hours. Chlorophyll was removed by incubating samples in 70% ethanol.

Toluidine Blue test

The Toluidine Blue (TB) test for the analysis of cuticular defects was performed as described in (Tanaka *et al.*, 2004). The first two leaves of soil grown 3-week-old plants or 15-day-old seedlings grown on MS-agar were stained at room temperature in an aqueous solution of 0.05% TB (Sigma) for 2-5 min. The TB solution was removed and samples were washed gently with distilled water until excess TB was removed. Samples were visualized under a LEICA stereo microscope (MZ10F) and photographed with a Leica DFC7000 T camera.

Chlorophyll leaching assay

The rate of chlorophyll loss was measured as described by Lolle *et al.* (1997). Rosettes from 3-week-old plants grown on soil were immersed in an 80% ethanol solution at room temperature and kept in the dark. Aliquots of the ethanol solution were removed at different intervals and the absorbance at 647, 664 and 537 nm was measured. Total chlorophyll concentration in rosettes was determined according to the technique described by Porra (2002). Complete rosettes were frozen in liquid nitrogen and grinded in a mortar. The powder (50 mg) was incubated for 12 hours at 4°C with 500 µL of a cold solution of acetone:Tris-HCl 1M, pH 8.0 (80:20). Samples were centrifuged and the absorbance of the supernatant was measured at 647, 664 and 537 nm.

The amount of chlorophyll (µmol) was calculated according to the formula reported by Sims and Gamon (2002): Chlorophyll a = 0.01373 A_{664} – 0.000897 A_{537} – 0.003046 A_{647}; Chlorophyll b = 0.02405 A_{647} – 0.004305 A_{537} – 0.005507 A_{664}, and was referred to rosette fresh weight.

DAPI Staining

To estimate the nuclear DNA content of trichomes, DAPI staining was performed mainly as described in Hülskamp *et al*. (1994). The first two leaves were collected once they were fully expanded and fixed in a 3.7% solution of formaldehyde in PBT (PBS with 0.1% Triton X-100) for 4 hours. Three 10-min washes were made with PBT and then samples were incubated in a PBT solution containing 1 µg/mL DAPI for 30 min followed by three washes with PBT. After two 15-min incubations in 80% ethanol to remove chlorophyll, samples were washed with PBT and stored in a 50% glycerol solution. The leaves were mounted in pure glycerol and observed in a NIKON Eclipse E200 fluorescence microscope. Pictures were taken using a NIKON D5300 digital camera and analyzed using the Fiji software (Schindelin *et al.*, 2012). For each genotype, total fluorescence of at least 50 nuclei was determined.

Chromatin immunoprecipitation

Chromatin immunoprecipitation (ChIP) assays were performed on 17-day-old whole rosettes expressing TCP15-GFP under the control of the *35SCaMV* promoter with anti-GFP (Abcam ab6556) and anti-IgG (Abcam ab6702) antibodies, mainly as described in Ariel et al. (2014). After cross-linking and extraction, chromatin was sonicated in a Bioruptor Pico water bath (Diagenode; 30 s on/30 s off pulses, at high intensity for 10 cycles, using Bioruptor microtubes). For immunoprecipitation, samples were incubated for 12 hours at 4°C with Protein A Dynabeads (Invitrogen) pre-coated with the corresponding antibodies. Immunoprecipitated DNA was recovered using phenol:chloroform:isoamyl alcohol mix (25:24:1, Sigma) followed by ethanol precipitation. Untreated sonicated chromatin was processed in parallel and considered the input sample. DNA was analyzed by qPCR using primers listed in Supplementary Table S1. Three biological replicates were performed with similar results for each ChIP-qPCR experiment.

Transcriptomics and functional genomics analyses

Processed microarray data from Oshima *et al*. (2013) were retrieved from NCBI (GSE31887) and differential gene expression was evaluated using the limma R package (Ritchie *et al*., 2015; version 3.36.5). p-values were FDR corrected. Finally, the log2 fold-changes of probes targeting the same gene were averaged and the p-values were combined with the Fisher's method. The Venn-like diagram was produced with the bvenn R package (Kolde, 2012). Data manipulation was performed with R (R Core Team, 2018).

Gene ontology enrichment analysis was performed with the topGO R package (Alexa and Rahnenfuhrer, 2016; version 2.32.0) using the *elim* method (Alexa *et al.*, 2006) and the Fisher test. No p-value correction was applied since the *elim* method controls for the dependency among nested parent-child GO categories, partially countering the dependency effects which are overcorrected by standard multiple-test p-value correction methods.

RESULTS

TCP14 and TCP15 regulate trichome branching in leaves and inflorescence stems

To analyze the specific role of TCP14 and TCP15 in the control of trichome branch development, we examined trichome morphology in the first two leaves of the *tcp14-4 tcp15-3* loss-of-function double mutant . This mutant was previously described by Kieffer *et al.* (2011) and contains very low amounts of truncated transcripts for *TCP14* and no detectable transcripts for *TCP15*. While 86% of trichomes in wild-type leaves showed three branches, and the rest showed only one or two branches, *tcp14-4 tcp15-3* leaves had 48% three-branched trichomes, 40% four-branched trichomes, and 10% five-branched trichomes (Fig. 1A, B). The increased proportion in overbranched trichomes in the mutant agrees with observations made with the repressive forms of TCP14 and TCP15 (Kieffer *et al.*, 2011; Li *et al.*, 2012) and confirm a role for *TCP14* and/or *TCP15* in trichome branch formation. To evaluate the individual contribution of each *TCP* gene, we analyzed trichome morphology in the *tcp14-6* (Kieffer *et al*., 2011) and the *tcp15-3* single mutants. We found that both mutants developed overbranched trichomes and that the proportion of trichomes with three, four and five branches was similar to that observed in the *tcp14-4 tcp15-3* double mutant (Fig. 1A, B). The average branch number per trichome of *tcp14* and *tcp15* simple and double mutants was 3.6, while the one of wild-type plants was 2.8 (Fig. 1C). These results suggest that both TCPs are required for the control of leaf trichome morphogenesis. In addition, the inflorescence stems of *tcp14-6* and *tcp15-3* plants showed 70% and 88% two-branched trichomes, respectively, in contrast with the trichomes of wild-type stems that were unbranched (Fig. 1D, E). The average branch number per trichome of *tcp14-6* and *tcp15-3* stems was then significantly higher than the one of wild-type stems (Fig. 1F). These results indicate that TCP14 and TCP15 are also involved in the regulation of trichome branching in stems.

TCP14 and TCP15 regulate the expression of MIXTA-like transcription factors

To gain insight into the molecular mechanism employed by the class I TCPs during the control of trichome branching, we looked for genes related to this process in a global expression analysis of plants that express a fusion of TCP15 to the EAR repressor motif under the control of the *TCP15* promoter (*pTCP15::TCP15-EAR* plants; Lucero *et al*., 2015) (Supplementary Table S2). We found that the expression of *MYB106/NOK* and *MYB16*, two related R2R3 MYB transcription factors that negatively regulate trichome branch formation (Folkers *et al.*, 1997; Jakoby *et al.*, 2008; Oshima *et al.*, 2013), was downregulated in *pTCP15::TCP15-EAR* plants (Fig. 2A). In addition, *CML42*, a calcium sensor whose mutation leads to overbranched trichomes in leaves (Dobney *et al.*, 2009), also appeared downregulated in these plants (Fig. 2A). To confirm the microarray results, we analyzed the expression of *MYB106*, *MYB16* and *CML42* in *pTCP15::TCP15-EAR* plants by reverse transcription followed by quantitative real-time PCR (RT-qPCR). We found that while expression of *CML42* was not significantly different from wild-type in the samples used for the analysis, the expression of *MYB106* and *MYB16* was significantly affected (Fig. 2B). In addition, *MYB106* and *MYB16* transcript levels were significantly increased in plants that ectopically express TCP15 (*35S::TCP15-RFP* plants; Viola *et al.*, 2016) compared to wild-type (Fig. 2C). To further analyze this, we crossed *35S::TCP15-RFP* plants with plants expressing the *uidA* (*gus*) reporter gene under the control of the *MYB106* or *MYB16* promoters (*pMYB106::GUS* and *pMYB16::GUS*, respectively). In a wild-type background, *MYB106* and *MYB16* promoter activity was detected at the base of emerging leaves and in trichomes (Fig. 2D). Activity of both promoters was considerably higher and extended to the whole lamina of developing leaves when *TCP15* was overexpressed (Fig. 2D), suggesting that TCP15 is able to induce the transcription of *MYB106* and *MYB16*. Increased expression of the *GUS* reporter gene in seedlings expressing *35S::TCP15-RFP* was also confirmed by RT-qPCR (Fig. 2E). Finally, we then analyzed transcript levels of the MYB transcription factor genes in total RNA isolated from the center of *tcp14-4 tcp15-3* mutant rosettes, containing very young leaves rich in developing trichomes (i.e. the sites of highest expression of these genes). *MYB106* transcript levels were significantly reduced in the *tcp14-4 tcp15-3* mutant compared to wild-type, while the results with *MYB16* did not reach statistical significance (Fig. 2F). The results indicate that TCP14 and TCP15 are required for the correct expression of *MYB106*. In the case of *MYB16*, it is possible that other class I TCPs are able to replace TCP14 and TCP15 when these are not present. This would explain why *MYB16*

expression is affected in *pTCP15::TCP15-EAR* and *35S::TCP15-RFP* plants, but not in the *tcp14-4 tcp15-3* mutant.

TCP15 binds to the *MYB106* promoter *in vivo*

Class I TCP transcription factors bind the motif GTGGGNCC (Viola *et al.*, 2011). We identified the sequence GTGGGGCC 1700 bp upstream of the transcription start site of *MYB106* (Supplementary Table S3), raising the possibility that TCP15 directly binds to the *MYB106* promoter. To investigate this, we performed a chromatin immunoprecipitation (ChIP) assay using chromatin extracted from *35S::TCP15-GFP* plants and anti-GFP antibodies. We found that three different genomic fragments of the *MYB106* promoter were enriched in comparison with the negative control gene *PP2A* (Fig. 2G). Moreover, the promoter fragment containing the TCP motif was the most enriched (Fig. 2G, fragment 2) in comparison with genomic fragments located either upstream or downstream in the promoter (Fig. 2G, fragments 1 and 3). The results indicate that TCP15 binds to the *MYB106* promoter *in vivo*, suggesting that *MYB106* may be a direct target of TCP15. Together with the presence of a TCP target site, the induction of *MYB106* promoter activity by TCP15 overexpression and the changes in *MYB106* transcript levels observed in *35S::TCP15-RFP* and *tcp14-4 tcp15-3* plants, these results suggest that TCP15 is most likely a direct positive regulator of *MYB106* expression. However, the existence of indirect regulation or the requirement of other proteins for promoter binding and activation cannot be ruled out.

TCP15 and MYB106 regulate common sets of genes

Our expression and phenotypic studies suggest that TCP15 and MYB106 may participate in common regulatory pathways during the control of trichome branching. Moreover, the reported expression patterns of *TCP15* and *MYB106* indicate that both genes are expressed in developing leaf primordia and trichomes (Jakoby *et al.*, 2008; Li *et al.*, 2012; Uberti-Manassero *et al.*, 2012). We then analyzed available microarray data for *pTCP15::TCP15-EAR* (Lucero *et al.*, 2015) and *35S::MYB106-EAR* plants (Oshima *et al.*, 2013) to evaluate possible common patterns of gene expression (Supplementary Table S2). A total of 1282 genes were differentially expressed in *pTCP15::TCP15-EAR* plants (at least two-fold expression change, p-value below 0.05), of which 740 were upregulated and 542 were downregulated. In *35S::MYB106-EAR* plants, differentially expressed genes amounted to 5605 (1888 genes upregulated and 3717 genes downregulated). A comparison of both sets of genes showed that 58.35% (748/1282) of the genes whose expression changed in

pTCP15::TCP15-EAR plants showed statistically significant expression changes in *35S::MYB106-EAR* plants (sum of overlapping genes in Fig. 3A). Interestingly, there was a significant overlap in genes regulated in the same direction in these plants, since 68.82% (373/542) of the genes downregulated in *pTCP15::TCP15-EAR* plants were also downregulated in *35S::MYB106-EAR* plants, while only 1.29% (7/542) of the genes repressed in *pTCP15::TCP15-EAR* plants were upregulated in *35S::MYB106-EAR* plants (Fig. 3A). In a similar way, 34.59% (256/740) of the upregulated genes in *pTCP15::TCP15-EAR* plants were also upregulated in *35S::MYB106-EAR* plants while 15.16% (112/740) were downregulated (Fig. 3A). Gene Ontology (GO) analysis of the group of 373 genes that were downregulated in both lines of plants showed enrichment in genes involved in xylan biosynthesis, auxin, brassinosteroids and cytokinin pathways, cell wall biosynthesis, and cuticle biosynthesis (Fig. 3B; Supplementary Table S4). For genes upregulated in both lines of plants, enrichment in stress responses, abscisic acid signaling, and also auxin responses, was observed (Fig. 3B; Supplementary Table S4). These data suggest that MYB106 and TCP15 may be involved in the regulation of similar processes.

TCP14, TCP15 and MYB106 affect endoreplication in trichome cells

After determination, the trichome progenitor cell stops division and switches to an endoreplication cycle, whereby successive rounds of full genome replication occur in the absence of mitosis. Endoreplication correlates with trichome growth and mutants with increased endoreplication often show increased trichome branching (Schellmann and Hülskamp, 2005). Previous studies showed that the trichomes of plants that express a dominant repressor form of TCP15 show increased nuclear DNA content (Li *et al*., 2012). To determine whether the mutants in MYB106 and the TCPs under study show altered endoreplication in trichomes, we estimated the nuclear DNA content of trichomes from *tcp14-4 tcp15-3* and *myb106-2* leaves by measuring the fluorescence intensity of nuclei stained with 4´,6-diamino-phenylindole (DAPI). This analysis, although not strictly quantitative, indicated that the DNA content of *tcp14-4 tcp15-3* and *myb106-2* trichomes was higher than the one of wild-type trichomes (Fig. 4A), suggesting that *tcp14-4 tcp15-3* and *myb106-2* trichomes undergo extra rounds of endoreplication. A cytological analysis using nuclei from isolated trichomes would be required to quantitatively assess this and determine the actual ploidy level of mutant trichome cells.

Endoreplication is controlled by several pathways, one of which depends on a reduction in the activity of the cell cycle regulatory genes *CYCA2;3*, *CYCB1;1* and *RBR* (Coelho *et al.*,

2005; Desvoyes *et al.*, 2006; Imai, 2006). Li *et al.* (2012) already reported that transcript levels of *CYCA2;3* and *RBR* were reduced in seedlings of plants expressing a repressor form of TCP15. We then analyzed changes observed in *tcp14-4 tcp15-3* and *myb106-2* mutants. As shown in Fig. 4B and C, transcript levels of *CYCA2;3*, *CYCB1;1* and *RBR* were reduced in both mutants compared with wild-type plants. These results suggest that, similar to TCP14 and TCP15, MYB106 modulates endoreplication cycles in trichomes possibly by affecting the expression of key cell cycle regulators.

MYB106 overexpression reduces the trichome branching phenotype of the _tcp14 tcp15_ mutant

Since *MYB106* is downregulated in the *tcp14-4 tcp15-3* mutant, we tested the effect of overexpressing *MYB106* on trichome development in the *tcp14-4 tcp15-3* mutant background For this, we first sought to obtain stable homozygous lines transformed with the *MYB106* coding region under the control of the *35SCaMV* promoter in a wild-type (Col-0) background. We selected from the T1 population of transformants three independent lines that overexpressed the transgene (Supplementary Fig. S2A) and reproduced them to obtain homozygotes. Notably, all the *35S::MYB106* T3 homozygous lines developed overbranched trichomes, similar to those of the *myb106-2* mutant. In addition, these lines showed low levels of *MYB106* transcripts (Supplementary Fig. S2B). This observation is consistent with a previous report indicating that expression of *MYB106* from the *35SCaMV* promoter caused increased trichome branching as a result of co-suppression of the transgene and the endogenous gene (Gilding and Marks, 2010). We then decided to analyze trichome morphology in the T1 population of wild-type and *tcp14-4 tcp15-3* plants transformed with the *35S::MYB106* construct to avoid any obvious gene silencing effect. Approximately half of the independent *35S::MYB106* T1 lines analyzed in wild-type background presented overbranched trichomes, indicating a silencing effect, and were discarded. In lines from the other half, a slight decrease in the proportion of three-branched trichomes and a concomitant increase in the proportion of two-branched trichomes was observed (Fig. 5A), but this did not reach statistical significance when the average number of branches per trichome was calculated (Fig. 5B). In *35S::MYB106* T1 lines in *tcp14-4 tcp15-3* background, we observed a decrease in the proportion of four-branched trichomes and an increase in three-branched trichomes compared with the *tcp14-4 tcp15-3* mutant (Fig. 5A; Supplementary Fig. S3), leading to a significant decrease in the average branch number per trichome (Fig. 5B). These results indicate that *MYB106* can partially overcome the defect in TCPs during trichome

branch development. In addition, the trichome branch phenotype of the *tcp15-3 myb106-2* double homozygous mutant was similar to that of *myb106-2* (Fig. 5C; D), suggesting that TCP15 acts in the same pathway as MYB106 during trichome branch formation. Altogether, the results suggest that TCP15 influences trichome branch formation through *MYB106*.

Considering the overlap observed in genes regulated by TCP15 and MYB106, we also assessed the effect of *TCP15* overexpression on the phenotype of the *myb106-2* mutant. Overexpression of TCP15-RFP in a wild-type background did not significantly modify the trichome morphology in the first pair of leaves and inflorescence stems (Supplementary Fig. S4A, B). In contrast, an effect on trichome morphology was evident when *35S::TCP15-RFP* plants were crossed with *myb106-2* mutant plants. While *myb106-2* leaves showed similar proportions of three-, four-, and five-branched trichomes and about 9% of trichomes with six branches (Supplementary Fig. S4A), introduction of the *35S::TCP15-RFP* construct in the *myb106-2* mutant caused an increase in three-branched trichomes to 52% along with a decrease of five-branched trichomes to 15% and the disappearance of trichomes with six branches (Supplementary Fig. S4A). This reduced the average branch number per trichome from 4.3 to 3.6 in leaves (Supplementary Fig. S4A, B). In the main inflorescence stem, the introduction of the *35S::TCP15-RFP* construct in *myb106-2* plants caused the development of the typical unbranched trichomes, which are rare in *myb106-2* stems, and the disappearance of three-branched trichomes (Supplementary Fig. S4C). In fact, the stems of *35S::TCP15-RFP myb106-2* plants showed a decrease in the average branch number per trichome to 1.7, compared with 2.5 for *myb106-2* plants (Supplementary Fig. S4D). These results indicate that TCP15 partially compensates *myb106* loss-of-function and suggest that TCP15 and MYB106 could regulate trichome branch formation in part through the regulation of similar groups of genes..

TCP14 and TCP15 affect cuticle permeability

In addition to the control of trichome branching, *MYB106* and *MYB16* were shown to regulate the expression of cutin biosynthesis and wax accumulation genes (Oshima *et al*., 2013). As described above, among the genes commonly downregulated in *pTCP15::TCP15-EAR* and *35S::MYB106-EAR* plants there was an enrichment in the categories “cuticle development” and “very long-chain fatty acid metabolic process” (Fig. 3B; Supplementary Table S4). For example, the expression of *CYP86A4* and *GPAT6*, which encode enzymes involved in the synthesis of cutin precursors (Li-Beisson *et al.*, 2009), of *LTPG2*, which encodes a LTPG protein involved in wax transport (Kim *et al.*, 2012), of the wax biosynthesis gene *CER2*, and

of the cutin synthase gene *CUS2* (Yeats and Rose, 2013; Yeats *et al.*, 2014; Hong *et al.*, 2017) was reduced in *pTCP15::TCP15-EAR* plants in comparison with wild-type plants (Fig. 6A; Supplementary Table S2). In addition, another transcription factor involved in cuticle development, *SHN2* (Shi *et al.*, 2011), was also downregulated in *pTCP15::TCP15-EAR* plants according to the microarray results (Fig. 6A; Supplementary Table S2). This prompted us to evaluate possible cuticle defects in plants with altered expression of the TCPs. We observed that toluidine blue, a hydrophilic dye that only penetrates plant surfaces with permeable cuticles (Tanaka *et al.*, 2004), rapidly stained leaves and flowers from *pTCP15::TCP15-EAR* plants (Fig. 6B), suggesting that these plants have a defective cuticle. We also found that *tcp14-6*, *tcp15-3*, *tcp14-4 tcp15-3* and *myb106-2* mutant leaves exhibited increased cuticle permeability compared with the wild-type (Fig. 6C). In addition, *tcp14-4 tcp15-3* and *myb106-2* mutant rosettes showed increased chlorophyll leaching when submerged in 80% ethanol (Fig. 6D), even though the initial chlorophyll content in these plants was similar to wild-type (Fig. 6E). The increased permeability to toluidine blue and chlorophyll leaching of the *tcp14-4 tcp15-3* mutant were suppressed when the *35S::TCP15-RFP* construct was introduced in these plants (Supplementary Fig. S5). These results suggest that TCP14 and TCP15 are required for correct cuticle formation.

Expression of cuticle biosynthesis genes is affected in *tcp14 tcp15* plants

To determine whether *tcp14-4 tcp15-3* plants show changes in the expression of cuticle biosynthesis genes, we performed a RT-qPCR analysis. We observed that expression of *CYP86A4*, *GPAT6* and *CUS2* was reduced in the *tcp14-4 tcp15-3* mutant in comparison with wild-type plants (Fig. 7A). In contrast, expression of *CER2* was only marginally affected (the results did not reach statistical significance) and that of *LTPG2* was not changed (Fig. 7A). Similar transcriptional changes were observed in *myb106-2* mutant plants (Fig. 7B). In addition, expression of *CYP86A4* and *CUS2* was significantly increased in *35S::TCP15-RFP* plants, while *GPAT6* transcript levels were only slightly increased and the expression of *CER2* was not affected (Fig. 7C). Since *MYB106* is a direct target of TCP15, one possibility is that the TCPs regulate the transcription of cuticle biosynthesis genes through the induction of *MYB106* expression. However, the analysis of the promoter regions of 53 genes previously reported to be involved in cuticle formation (Javelle *et al.*, 2011; Yang *et al.*, 2012; Yeats and Rose, 2013; Fich *et al.*, 2016) indicated that 25 of them have TCP binding motifs (Supplementary Table S3). Remarkably, among these 25 genes, *CYP86A4*, *CYP86A7*, *GPAT3*, *GPAT6*, *GPAT8*, and *CUS2* showed reduced expression in either *pTCP15::TCP15-*

EAR (Supplementary Table S2) or *tcp14-4 tcp15-3* plants. This suggests that these genes could be direct targets of the TCPs. We then selected *CUS2* as a representative gene to perform a ChIP assay with plants that express GFP-tagged TCP15. Consistent with our hypothesis, a promoter fragment spanning the *CUS2* promoter region that contains the putative TCP binding motif (GGGACCT, located at about -1000 bp from the transcriptional start) was preferentially immunoprecipitated in comparison with other genomic fragments located either upstream or downstream and with the control gene *PP2A* (Fig. 7D; Supplementary Fig. S6). Binding to the *CUS2* promoter *in vivo* and the presence of a TCP binding motif suggest that, in addition to an indirect regulation through MYB106, TCP15 and other TCPs may directly regulate the expression of *CUS2* and, possibly, other cuticle biosynthesis genes.

TCP15 modulates the expression of the transcriptional regulator of cuticle biosynthesis SHN1

In addition to *MYB106* and *MYB16*, we observed that the gene encoding the AP2/EREBP transcription factor *SHN2* was also repressed in *pTCP15::TCP15-EAR* plants (Fig. 6A). SHN2 belongs to the small clade of SHINE transcription factors that directly activate the transcription of several cutin biosynthesis genes and influence wax biosynthesis (Aharoni *et al.*, 2004; Shi *et al.*, 2011). RT-qPCR analysis indicated that not only *SHN2*, but also *SHN1* transcript levels were decreased in *tcp14-4 tcp15*-3 plants compared with wild-type (Fig. 7E). Conversely, the expression of *SHN1* and *SHN2* was increased in *35S::TCP15-RFP* plants (Fig. 7F). The *SHN1* promoter contains two closely located TCP motifs (TGGGTCCA and TGGGTCCC) about 800 bp upstream from the transcription start site (Supplementary Table S3), suggesting that it may be a direct target of TCP proteins. Indeed, ChIP-qPCR analyses with primers flanking the TCP binding sites in the *SHN1* promoter showed that TCP15 binds to this region (Fig. 7G; Supplementary Fig. S6). The results suggest that TCP15 may regulate the expression of *SHN1* through direct binding to TCP binding motifs present in its promoter. Notably, *SHN1* is also regulated by MYB106 (Oshima *et al.*, 2013). Thus, as discussed for cuticle biosynthesis genes, TCP15 may also regulate *SHN1* expression through MYB106. The close crosstalk between these TCP, MYB and AP2/EREBP transcription factors is reflected by the fact that a common set of genes is downregulated in *pTCP15::TCP15-EAR* (Lucero *et al.*, 2015), *35S::MYB106-EAR* and *35S::SHN1-EAR* plants (Oshima *et al.*, 2013) (Supplementary Fig. S7A; Supplementary Table S2). GO analysis of this set of genes showed

enrichment in terms as “cuticle development”, “cell wall biogenesis” and “cutin biosynthetic process” (Supplementary Fig. S7B; Supplementary Table S4).

DISCUSSION

The epidermal layer of the aboveground parts of plants is a multifunctional tissue involved in a number of processes, including osmotic regulation, pollinator attraction and defense. To optimally perform these functions, cells of the epidermis are differentiated into a variety of cell types (e.g. pavement cells, trichomes, and stomata guard cells). This tissue also develops a unique cell wall that not merely contains cellulose, hemicellulose, pectins, and proteins but also a cuticular matrix, which is largely composed of cutin embedded and overlaid with waxes (Yeats and Rose, 2013). The cuticle provides a waterproof barrier between epidermal cells and the external environment (Riederer and Müller, 2006) and, along with the specialized cells of the epidermis, plays an important role during organ development as well as in the protection against biotic and abiotic stresses (Wagner *et al.*, 2004; Bargel *et al.*, 2006). In this study, we found that the class I TCP transcription factors TCP14 and TCP15 from *Arabidopsis thaliana* act as regulators of aerial epidermis development and specialization. Leaves and inflorescence stems of *tcp14-6* and *tcp15-3* single mutants develop trichome cells with increased number of branches and show a defective cuticle (Figs. 1 and 6). The *MIXTA-like* genes *MYB106* and *MYB16* are R2R3 MYB transcription factors that also regulate trichome branching and cuticle development (Folkers *et al.*, 1997; Jakoby *et al.*, 2008; Oshima *et al.*, 2013) and global expression analyses indicated that TCP15 and MYB106 regulate common sets of genes (Fig. 3). This suggests the existence of a functional connection between these transcription factors. Indeed, *MYB106* expression is reduced in the *tcp14-4 tcp15-3* mutant and both *MIXTA-like* genes are repressed in *pTCP15::TCP15-EAR* plants (where the action of other redundant TCPs is hindered by the expression of a dominant repressor form of TCP15), indicating that *MYB106* and *MYB16* are regulated by TCP15 (Fig. 2). This is also evidenced by the fact that TCP15 overexpression activates the promoters of both *MIXTA-like* genes. Moreover, we showed that TCP15 binds *in vivo* to a region of the *MYB106* promoter containing a TCP binding motif, indicating that TCP15 may directly regulate *MYB106* transcription (Fig. 2). In agreement with this, introduction of the *tcp15-3* mutation in the *myb106-2* mutant background does not enhance trichome branching and the increase in trichome branch number caused by a loss-of-function of *TCP14* and *TCP15* is partly overcome by *MYB106* overexpression (Fig. 5). Even if we did not investigate further the role of TCP14, the increased trichome branching and cuticle permeability evidenced by

the *tcp14-6* mutant suggest that TCP14 may act in a similar pathway as TCP15. Thus, we propose that TCP15 and other class I TCPs, like TCP14, influence trichome branch ramification, at least in part, through the regulation of the expression of *MIXTA-like* genes. As MYB16 does not have a consensus TCP binding motif in its promoter, it seems that the TCPs would regulate indirectly the expression of *MYB16*.

Studies on various trichome mutants have shown that a change in the endoreplication status alters the trichome branching phenotype (Hülskamp, 2004). There are reports showing that class I TCPs regulate endoreplication either positively (Zhang *et al.*, 2019) or negatively (Peng *et al.*, 2015) to control hypocotyl and leaf development. In addition, expression of a repressor form of TCP15 increases trichome branch number and endoreplication (Li *et al.*, 2012). In this study, we found that trichome cells of *tcp14-4 tcp15-3* and *myb106-2* plants have increased DNA content (Fig. 4), suggesting that the TCPs and MYB106 influence trichome branching through the inhibition of endoreplication. In fact, expression of *CYCA2*;3, *CYCB1;1* and *RBR1*, which are negative regulators of endoreplication (Edgar *et al.*, 2014), is affected in these mutants (Fig. 4). Previous studies suggesting that TCP15 directly regulates *CYCA2;3* and *RBR1* expression to repress endoreplication (Li *et al*., 2012) are in agreement with our findings. In the case of MYB106, previous reports are ambiguous. From initial studies performed by Folkers *et al*. (1997) it has been assumed that *MYB106* belongs to the group of genes that regulate trichome branching in an endoreplication-independent pathway. In turn, Gilding and Marks (2010) found that the nuclei of a *myb106* mutant have increased DNA content. Our results agree with those of Gilding and Marks (2010), indicating that the observed branching defects in *myb106-2* trichomes may be caused by an alteration in endoreplication. However, *myb106-2* plants exhibit a more severe trichome phenotype than *tcp14-4 tcp15-3* plants even if their DNA content appears to be similar, raising the possibility that MYB106 also acts in an endoreplication-independent pathway. Recently, it has been reported that the miR319-regulated class II TCP proteins suppress trichome branching in leaves and inflorescence stems from *Arabidopsis* by direct transcriptional activation of *GLABROUS INFLORESCENCE STEMS* (*GIS*), described as a transcription factor that inhibits trichome branching by endoreplication-independent pathways (An *et al.*, 2012; Vadde *et al.*, 2018). We did not observe changes in *GIS* expression in *tcp14-4 tcp15-3* and *pTCP15::TCP15-EAR* plants. Then, TCPs from both classes act as negative regulators of trichome branching in *Arabidopsis* but the molecular mechanisms involved seem to be different. While class II proteins modulate trichome branching through the control of *GIS*

expression, class I proteins do so through the activation of the expression of *MIXTA-like* genes and cell cycle regulators that inhibit the entry into endoreplication cycles.

The expression of repressor versions of MYB106 and MYB16 generates a defective cuticle in leaves and flowers as a consequence of a decrease in the expression of genes associated with cutin and wax biosynthesis, e.g. *CYP86A4*, *LACS2* and *CER2* (Oshima *et al*., 2013). This led us to analyze cuticle permeability in plants defective in the function of TCP14 and TCP15. Our results suggest that these class I TCPs are also necessary for correct cuticle formation (Fig. 6). In addition, it has been proposed that MYB106 directly regulates the activity of the *SHN1* and *CYP86A4* promoters (Oshima *et al*., 2013). *MYB106*, *SHN1* and *CYP86A4* are downregulated in *tcp14-4 tcp15-3* plants (Fig 7). This reinforces the idea that the functions of class I TCPs and MIXTA-like transcription factors are closely interconnected. Moreover, we found that several genes associated with cuticle development present one or more TCP binding motifs in their promoter sequences, suggesting that genes involved in cuticle formation may be direct targets of class I TCPs. For one of these genes, *CUS2*, we confirmed that TCP15 binds to the region of the promoter containing the TCP binding motif (Fig. 7). In addition, we found that the TCPs under study are required for the expression of *SHN1* and *SHN2*, which belong to a small clade of transcriptional regulators of cutin and wax biosynthesis genes (Aharoni *et al.*, 2004), and that TCP15 binds to a region containing two TCP binding motifs in the *SHN1* promoter (Fig. 7). Altogether, our results indicate that class I TCP transcription factors modulate the expression of genes involved in cuticle formation acting at different levels: through MYB106, which in turn modulates the expression of SHN transcription factors (Oshima *et al*., 2013), through SHN1, which together with other *SHN* transcription factors promote lipid biosynthesis (Aharoni *et al.*, 2004; Broun *et al.*, 2004), and through regulation of genes involved in the cuticle biosynthesis pathway. Decreased expression of these genes would be the cause of the increased permeability observed in plants with defective function of TCP14 and TCP15. The actual changes in cuticle composition brought about by a deficiency in these TCPs would give more information about the pathways that are specifically affected.

In summary, our study reveals new roles for class I TCP transcription factors as coordinators of aerial epidermal tissue specialization, most likely acting through direct and indirect regulation of the expression of MIXTA-like and SHN transcription factors, and of cell-cycle and cuticle biosynthesis genes (Fig. 8).

ACCESSION NUMBERS

Sequence data from this article can be found in the Arabidopsis TAIR database under the following accession numbers: *TCP15*, At1g69690; *TCP14*, At3g47620; *CYCA2;3*, At1g15570; *CYCB1;1*, At4g37490; *RBR1*, At3g12280; *CML42*, At4g20780; *MYB106*, At3g01140; *MYB16*, At5g15310; *SHN1*, At1g15360; *SHN2*, At5g11190; *CER2*, At4g24510; *CUS2*, At5g33370; *CYP86A4*, At1g01600; *GPAT6*, At2g38110; *LTPG2*, At3g43720.

ACKNOWLEDGMENTS

We thank Drs. Martin Kieffer (University of Leeds, UK), Nobutaka Mitsuda (National Institute of Advanced Industrial Science and Technology, Japan), and the Arabidopsis Biological Resource Center (Ohio State University) for kindly providing seeds used in this study. We also thank Lucía Ferrero for the *35S::TCP15-GFP* plants and Florencia Rivarosa for help with the crosses of the reporter lines.

FUNDING

This work was supported by grants from ANPCyT (Agencia Nacional de Promoción Científica y Tecnológica, Argentina), CONICET (Consejo Nacional de Investigaciones Científicas y Técnicas, Argentina) and Universidad Nacional del Litoral. ILV, DHG, AA and FA are members of CONICET. AC is a CONICET fellow.

Conflict of interest

The authors declare no conflict of interest.

REFERENCES

Aharoni A, Dixit S, Jetter R, Thoenes E, Arkel G van, Pereira A. 2004. The SHINE Clade of AP2 Domain Transcription Factors Activates Wax Biosynthesis, Alters Cuticle Properties, and Confers Drought Tolerance when Overexpressed in Arabidopsis. The Plant Cell **16**, 2463–2480.

Alexa A, Rahnenfuhrer J. 2016. topGO: Enrichment Analysis for Gene Ontology. R package version 2.32.0.

Alexa A, Rahnenfuhrer J, Lengauer T. 2006. Improved scoring of functional groups from gene expression data by decorrelating GO graph structure. Bioinformatics **22**, 1600–1607.

An L, Zhou Z, Su S, Yan A, Gan Y. 2012. GLABROUS INFLORESCENCE STEMS (GIS) is required for trichome branching through gibberellic acid signaling in arabidopsis. Plant and Cell Physiology **53**, 457–469.

Ariel F, Jegu T, Latrasse D, Romero-barrios N, Christ A, Benhamed M, Crespi M. 2014. Noncoding Transcription by Alternative RNA Polymerases Dynamically Regulates an Auxin-Driven Chromatin Loop. Molecular Cell, 383–396.

Bargel H, Koch K, Cerman Z, Neinhuis C. 2006. Structure–function relationships of the plant cuticle and cuticular waxes — a smart material? Functional Plant Biology **33**, 893.

Broun P, Poindexter P, Osborne E, Jiang C-Z, Riechmann JL. 2004. WIN1, a transcriptional activator of epidermal wax accumulation in Arabidopsis. Proceedings of the National Academy of Sciences **101**, 4706–4711.

Charrier B, Champion A, Henry Y, Kreis M. 2002. Expression Profiling of the Whole Arabidopsis Shaggy- Like Kinase Multigene Family by Real-Time Reverse. Plant Physiology **130**, 577–590.

Clough SJ, Bent AF. 1999. Floral dip : a simplified method for Agrobacterium-mediated transformation of Arabidopsis thaliana. The Plant Journal **16**, 735–743.

Coelho CM, Dante RA, Sabelli PA, Sun Y, Dilkes BP, Gordon-kamm WJ, Larkins BA, Sciences P, Arizona CMC. 2005. Cyclin-Dependent Kinase Inhibitors in Maize Endosperm and Their Potential Role in Endoreduplication 1. Plant Physiology **138**, 2323–2336.

Cominelli E, Sala T, Calvi D, Gusmaroli G, Tonelli C. 2008. Over-expression of the Arabidopsis AtMYB41 gene alters cell expansion and leaf surface permeability. The Plant Journal, 53–64.

Cubas P, Lauter N, Doebley J, Coen E. 1999. The TCP domain: A motif found in proteins regulating plant growth and development. Plant Journal **18**, 215–222.

Danisman S. 2016. TCP Transcription Factors at the Interface between Environmental

Challenges and the Plant ' s Growth Responses. Frontiers in Plant Science **7**, 1–13.

Davière JM, Wild M, Regnault T, Baumberger N, Eisler H, Genschik P, Achard P. 2014. Class i TCP-DELLA interactions in inflorescence shoot apex determine plant height. Current Biology **24**, 1923–1928.

Desvoyes B, Ramirez-parra E, Xie Q, Chua N, Gutierrez C. 2006. Cell Type-Specific Role of the Retinoblastoma / E2F Pathway during Arabidopsis Leaf Development 1. Plant Physiology **140**, 67–80.

Dobney S, Chiasson D, Lam P, Smith SP, Snedden WA. 2009. The calmodulin-related calcium sensor CML42 plays a role in trichome branching. Journal of Biological Chemistry **284**, 31647–31657.

Edgar BA, Zielke N, Gutierrez C. 2014. Endocycles: a recurrent evolutionary innovation for post-mitotic cell growth. Nature Reviews Molecular Cell Biology **15**, 197–210.

Ferrero L V, Viola IL, Ariel FD, Gonzalez DH. 2019. Class I TCP Transcription Factors Target the Gibberellin Biosynthesis Gene GA20ox1 and the Growth-Promoting Genes HBI1 and PRE6 during Thermomorphogenic Growth in Arabidopsis. Plant and Cell Physiology **60**, 1633–1645.

Fich EA, Segerson NA, Rose JKC. 2016. The Plant Polyester Cutin: Biosynthesis, Structure, and Biological Roles. Annual Review of Plant Biology **67**, 207–233.

Folkers U, Berger J, Hülskamp M. 1997. Cell morphogenesis of trichomes in *Arabidopsis*: differential control of primary and secondary branching by branch initiation regulators and cell growth. Development **124**, 3779–3786.

Gilding EK, Marks MD. 2010. Analysis of purified glabra3-shapeshifter trichomes reveals a role for NOECK in regulating early trichome morphogenic events. Plant Journal **64**, 304–317.

Hellens RP, Anne Edwards E, Leyland NR, Bean S, Mullineaux PM. 2000. pGreen: A versatile and flexible binary Ti vector for Agrobacterium-mediated plant transformation. Plant Molecular Biology **42**, 819–832.

Hiratsu K, Matsui K, Koyama T, Ohme-Takagi M. 2003. Dominant repression of target genes by chimeric repressors that include the EAR motif, a repression domain, in Arabidopsis. Plant Journal **34**, 733–739.

Hong L, Brown J, Segerson NA, Rose JKC, Roeder AHK. 2017. CUTIN SYNTHASE 2 Maintains Progressively Developing Cuticular Ridges in Arabidopsis Sepals. Molecular Plant **10**, 560–574.

Hülskamp M. 2004. Plant trichomes: A model for cell differentiation. Nature Reviews

Molecular Cell Biology **5**, 471–480.

Hülskamp M, Miséra S, Jürgens G. 1994. Genetic dissection of trichome cell development in Arabidopsis. Cell **76**, 555–566.

Imai KK. 2006. The A-Type Cyclin CYCA2;3 Is a Key Regulator of Ploidy Levels in Arabidopsis Endoreduplication. the Plant Cell Online **18**, 382–396.

Jakoby MJ, Falkenhan D, Mader MT, Brininstool G, Wischnitzki E, Platz N, Hudson A, Hulskamp M, Larkin J, Schnittger A. 2008. Transcriptional Profiling of Mature Arabidopsis Trichomes Reveals That NOECK Encodes the MIXTA-Like Transcriptional Regulator MYB106. Plant Physiology **148**, 1583–1602.

Javelle M, Vernoud V, Rogowsky PM, Ingram GC. 2011. Epidermis: The formation and functions of a fundamental plant tissue. New Phytologist **189**, 17–39.

Kieffer M, Master V, Waites R, Davies B. 2011. TCP14 and TCP15 affect internode length and leaf shape in Arabidopsis. Plant Journal **68**, 147–158.

Kim H, Lee SB, Kim HJ, Min MK, Hwang I, Suh MC. 2012. Characterization of glycosylphosphatidylinositol-anchored lipid transfer protein 2 (LTPG2) and overlapping function between LTPG/LTPG1 and LTPG2 in cuticular wax export or accumulation in arabidopsis thaliana. Plant and Cell Physiology **53**, 1391–1403.

Kolde R. 2012. bvenn: A Simple alternative to proportional Venn diagrams. R package version 0.1.

Li-Beisson Y, Pollard M, Sauveplane V, Pinot F, Ohlrogge J, Beisson F. 2009. Nanoridges that characterize the surface morphology of flowers require the synthesis of cutin polyester. Proceedings of the National Academy of Sciences **106**, 22008–22013.

Li-beisson Y, Shorrosh B, Beisson F, *et al.* 2013. Acyl-Lipid Metabolism.

Li M, Chen H, Chen J, Chang M, Palmer IA, Gassmann W. 2018. TCP Transcription Factors Interact With NPR1 and Contribute Redundantly to Systemic Acquired Resistance. Frontiers in Plant Science **9**, 1–12.

Li ZY, Li B, Dong AW. 2012. The arabidopsis transcription factor AtTCP15 regulates endoreduplication by modulating expression of key cell-cycle genes. Molecular Plant **5**, 270–280.

Lolle SJ, Berlyn GP, Engstrom EM, Krolikowski KA, Reiter W-DD, Pruitt RE. 1997. Developmental regulation of cell interactions in the Arabidopsis fiddlehead-1 mutant: a role for the epidermal cell wall and cuticle. Developmental biology **189**, 311–21.

Lucero LE, Manavella PA, Gras DE, Ariel FD, Gonzalez DH. 2017. Class I and Class II TCP Transcription Factors Modulate SOC1-Dependent Flowering at Multiple Levels.

Molecular Plant **10**, 1571–1574.

Lucero LE, Uberti-Manassero NG, Arce AL, Colombatti F, Alemano SG, Gonzalez DH. 2015. TCP15 modulates cytokinin and auxin responses during gynoecium development in Arabidopsis. The Plant Journal **84**, 267–282.

Mathur J. 2006. Trichome cell morphogenesis in *Arabidopsis*: a continuum of cellular decisionsThis review is one of a selection of papers published in the Special Issue on Plant Cell Biology. Canadian Journal of Botany **84**, 604–612.

Mauricio R, Rausher MD. 1997. Experimental manipulation of putative selective agents provides evidence for the role of natural enemies in the evolution of plant defense. Evolution **51**, 1435–1444.

Nicolas M, Cubas P. 2016. TCP factors: new kids on the signaling block. Current Opinion in Plant Biology **33**, 33–41.

Oshima Y, Mitsuda N. 2013. The MIXTA-like transcription factor MYB16 is a major regulator of cuticle formation in vegetative organs. Plant Signaling and Behavior **8**, 14–17.

Oshima Y, Shikata M, Koyama T, Ohtsubo N, Mitsuda N, Ohme-Takagi M. 2013. MIXTA-Like Transcription Factors and WAX INDUCER1/SHINE1 Coordinately Regulate Cuticle Development in *Arabidopsis* and *Torenia fournieri*. The Plant Cell **25**, 1609–1624.

Peng Y, Chen L, Lu Y, Wu Y, Dumenil J, Zhu Z, Bevan MW, Li Y. 2015. The Ubiquitin Receptors DA1, DAR1, and DAR2 Redundantly Regulate Endoreduplication by Modulating the Stability of TCP14/15 in Arabidopsis. The Plant Cell **27**, 649–662.

Pollard M, Beisson F, Li Y, Ohlrogge JB. 2008. Building lipid barriers: biosynthesis of cutin and suberin. Trends in Plant Science **13**, 236–246.

Porra RJ. 2002. The chequered history of the development and use of simultaneous equations for the accurate determination of chlorophylls a and b. Photosynthesis Research **73**, 149–156.

R Core Team. 2018. R: A language and environment for statistical computing.

Raffaele S, Vailleau F, Léger A, Joubès J, Miersch O, Huard C, Blée E, Mongrand S, Domergue F, Roby D. 2008. A MYB Transcription Factor Regulates Very-Long-Chain Fatty Acid Biosynthesis for Activation of the Hypersensitive Cell Death Response in Arabidopsis. THE PLANT CELL **20**, 752–767.

Riederer M, Müller C. 2006. Biology of the Plant Cuticle. Annual Plant Reviews.1–10.

Ritchie ME, Phipson B, Wu D, Hu Y, Law CW, Shi W, Smyth GK. 2015. limma powers differential expression analyses for RNA-sequencing and microarray studies. Nucleic Acids Research **43**, e47 1-13.

Samuels L, Kunst L, Jetter R. 2008. Sealing Plant Surfaces: Cuticular Wax Formation by Epidermal Cells. Annual Review of Plant Biology **59**, 683–707.

Schellmann S, Hülskamp M. 2005. Epidermal differentiation: Trichomes in Arabidopsis as a model system. International Journal of Developmental Biology **49**, 579–584.

Schindelin J, Arganda-Carreras I, Frise E, *et al.* 2012. Fiji: An open-source platform for biological-image analysis. Nature Methods **9**, 676–682.

Seo PJ, Lee SB, Suh MC, Park M-J, Go YS, Park C-M. 2011. The MYB96 Transcription Factor Regulates Cuticular Wax Biosynthesis under Drought Conditions in Arabidopsis. The Plant Cell **23**, 1138–1152.

Serna L, Martin C. 2006. Trichomes: different regulatory networks lead to convergent structures. Trends in Plant Science **11**, 274–280.

Shi JX, Malitsky S, de Oliveira S, Branigan C, Franke RB, Schreiber L, Aharoni A. 2011. SHINE transcription factors act redundantly to pattern the archetypal surface of arabidopsis flower organs. PLoS Genetics **7**, e1001388.

Sims DA, Gamon JA. 2002. Relationships between leaf pigment content and spectral reflectance across a wide range of species, leaf structures and developmental stages. Remote Sensing of Environment **81**, 337–354.

Stracke R, Werber M, Weisshaar B. 2001. The R2R3-MYB gene family in Arabidopsis thaliana. Current Opinion in Plant Biology **4**, 447–456.

Tanaka T, Tanaka H, Machida C, Watanabe M, Machida Y. 2004. A new method for rapid visualization of defects in leaf cuticle reveals five intrinsic patterns of surface defects in Arabidopsis. Plant Journal **37**, 139–146.

Telfer A, Bollman KM, Poethig RS. 1997. Phase change and the regulation of trichome distribution in Arabidopsis thaliana. Development (Cambridge, England) **124**, 645–654.

Tian N, Liu F, Wang P, Zhang X, Li X, Wu G. 2017. The molecular basis of glandular trichome development and secondary metabolism in plants. Plant Gene **12**, 1–12.

Uberti-Manassero NG, Lucero LE, Viola IL, Vegetti AC, Gonzalez DH. 2012. The class i protein AtTCP15 modulates plant development through a pathway that overlaps with the one affected by CIN-like TCP proteins. Journal of Experimental Botany **63**, 809–823.

Vadde BVL, Challa KR, Nath U. 2018. The TCP4 transcription factor regulates trichome cell differentiation by directly activating *GLABROUS INFLORESCENCE STEMS* in *Arabidopsis thaliana*. The Plant Journal **93**, 259–269.

Viola IL, Camoirano A, Gonzalez DH. 2016. Redox-dependent modulation of anthocyanin biosynthesis by the TCP transcription factor TCP15 during exposure to high light intensity

conditions in arabidopsis. Plant Physiology **170**, 74–85.

Viola IL, Uberti Manassero NG, Ripoll R, Gonzalez DH. 2011. The *Arabidopsis* class I TCP transcription factor AtTCP11 is a developmental regulator with distinct DNA-binding properties due to the presence of a threonine residue at position 15 of the TCP domain. Biochemical Journal **435**, 143–155.

Vitha S. 2012. Histochemical localization of β-glucuronidase (GUS) reporter activity in plant tissues. Imaging, 1–6.

Wagner GJ, Wang E, Shepherd RW. 2004. New approaches for studying and exploiting an old protuberance, the plant trichome. Annals of Botany **93**, 3–11.

Xiao K, Mao X, Lin Y. 2017. Trichome, a Functional Diversity Phenotype in Plant. Molecular Biology **6**, 1–6, 1000183.

Yang W, Simpson JP, Li-Beisson Y, Beisson F, Pollard M, Ohlrogge JB. 2012. A land-plant-specific glycerol-3-phosphate acyltransferase family in Arabidopsis: substrate specificity, sn-2 preference, and evolution. Plant physiology **160**, 638–52.

Yeats TH, Huang W, Chatterjee S, Viart HMF, Clausen MH, Stark RE, Rose JKC. 2014. Tomato Cutin Deficient 1 (CD1) and putative orthologs comprise an ancient family of cutin synthase-like (CUS) proteins that are conserved among land plants. Plant Journal **77**, 667–675.

Yeats TH, Rose JKC. 2013. The Formation and Function of Plant Cuticles. Plant Physiology **163**, 5–20.

Zhang G, Zhao H, Chunguang Z, *et al.* 2019. Arabidopsis TCP7 Functions Redundantly with Other Class I TCPs to Regulate Endoreplication. Journal of Integrative Plant Biology.

FIGURE LEGENDS

Fig. 1. Trichome branching phenotype of *TCP14* and *TCP15* loss-of-function plants. (A) Representative images of the adaxial trichomes on the first two leaves of wild-type (wt), *tcp14-4 tcp15-3*, *tcp14-6* and *tcp15-3* plants. Scale bars: 0.2 mm. (B) Number of branches in adaxial trichomes of the first two leaves from wild-type (wt), *tcp14-4 tcp15-3*, *tcp14-6* and *tcp15-3* plants (n = 493, 536, 378 and 545, respectively). (C) Average branch number per trichome (branching index) calculated from the data in B. (D) Representative images of main

inflorescence stems of wild-type (wt), *tcp14-6* and *tcp15-3* plants. Scale bars: 2 mm. (E) Number of branches in main inflorescence stem trichomes of wild-type (wt), *tcp14-6* and *tcp15-3* plants (n = 238, 206 and 184, respectively). (F) Average branch number per trichome (branching index) calculated from the data in E. Trichomes of 8 plants were counted for each genotype. In (B), (C), (E) and (F), the bars indicate the mean ± SD of three biological replicates. Asterisks indicate significant differences compared to wild-type ($P < 0.05$; ANOVA).

Fig. 2. TCP15 regulates the expression of *MYB106* and *MYB16* MIXTA-like transcription factors. (A) Expression changes of *CML42*, *MYB106* and *MYB16*, involved in trichome branching, according to a global expression analysis performed in *pTCP15::TCP15-EAR* plants. LogFC: log2 of the fold-change in expression in *pTCP15:TCP15-EAR* plants relative to wild-type (wt) plants. Details are given in Supplementary Table S2. (B) Relative transcript levels of *CML42*, *MYB106* and *MYB16* in rosettes from wild-type (wt) and *pTCP15::TCP15-EAR* three-week-old plants. (C) Relative *MYB106* and *MYB16* transcript levels in developing leaves of wild-type (wt) and *35S::TCP15-RFP* plants. (D) Histochemical analysis of GUS activity in 15-day-old plants carrying the *pMYB106::GUS* and *pMYB16::GUS* reporters in a wild-type or a *35S::TCP15-RFP* background. Representative images of 10 plants analyzed for each line are shown. Scale bars: 0.5 mm. (E) Relative *GUS* transcript levels in 15-day-old plants carrying the *pMYB106::GUS* and *pMYB16::GUS* constructs in a wild-type (wt) or a *35S::TCP15-RFP* background. (F) Relative *MYB106* and *MYB16* transcript levels in developing leaves of wild-type (wt) and *tcp15-3 tcp14-4* plants. (G) ChIP-qPCR analysis showing the interaction of TCP15 with different chromatin regions of *MYB106*. The diagram on top depicts the *MYB106* gene with exons shown as black boxes. The position of the TCP motif (TCP box) and the three regions that were analyzed by ChIP-qPCR are indicated. *PP2A* was used as a negative control. The results show the mean ± SD of three technical replicates. The ChIP-qPCR experiment was repeated twice with similar results. The results of these repetitions are shown in Supplementary Fig. S1. In (B), (C), (E) and (F), the bars indicate the mean ± SD of three biological replicates. Asterisks indicate significant differences compared to wild-type ($P < 0.05$; Student´s *t* test).

Fig. 3. Genes with altered expression in *pTCP15::TCP15-EAR* and *35S::MYB106-EAR* plants overlap extensively. (A) Venn diagram showing down- and up-regulated genes in *pTCP15::TCP15-EAR* and *35S::MYB106-EAR* plants. (B) Gene Ontology (GO) analysis of

genes either down- or upregulated in both *pTCP15::TCP15-EAR* and *35S::MYB106-EAR* plants.

Fig. 4. TCP14, TCP15 and MYB106 inhibit endoreplication in trichome nuclei. (A) Fluorescence intensity of *in situ* DAPI-stained trichome nuclei of the first pair of leaves from wild-type, *tcp14-4 tcp15-3* and *myb106-2* plants. The graph shows the distribution of fluorescence intensities (as relative fluorescence units, RFU) in nuclei (n = 50 from at least 6 plants) from the different lines analyzed. A value of 32 RFU was arbitrarily assigned to the mean fluorescence intensity of wild-type trichome nuclei. (B) and (C), *CYCA2;3*, *CYCB1;1* and *RBR* transcript levels in *tcp14-4 tcp15-3* (B) and *myb106-2* (C) mutants relative to wild-type (wt) plants. The bars indicate the mean ± SD of three biological replicates. Asterisks indicate significant differences compared to wild-type ($P < 0.05$; Student´s *t* test).

Fig. 5. *35SCaMV* promoter-driven expression of MYB106 partially rescues trichome branch defects in *tcp14-4 tcp15-3* plants. (A) Trichome branch numbers in the first two leaves of wild-type (wt), *tcp14-4 tcp15-3,* and T1 *35S::MYB106* lines in wild-type and *tcp14-4 tcp15-3* backgrounds. The graph shows the mean ± SD of 10 plants for the wild-type and the *tcp14-4 tcp15-3* double mutant (674 and 731 trichomes analyzed, respectively), and of 4 independent T1 lines of *35S::MYB106* transformants (226 and 128 trichomes analyzed for lines in wild-type and *tcp14-4 tcp15-3* backgrounds, respectively). The experiment was repeated twice with similar results. (B) Average branch number per trichome (branching index) calculated from the data in A. (C) Number of branches in leaf adaxial trichomes from wild-type (wt), *tcp15-3*, *myb106-2* and *tcp15-3 myb106-2* plants (n = 374, 714, 563 and 545, respectively). Trichomes of 6-8 plants were counted for each genotype. The bars indicate the mean ± SD of three biological replicates. (D) Average branch number per trichome (branching index) calculated from the data in C. The bars indicate the mean ± SD of three biological replicates. In (A) and (C), asterisks indicate significant differences compared to wild-type ($P < 0.05$; ANOVA). In (B) and (D), different letters indicate significant differences ($P < 0.05$; ANOVA).

Fig. 6. Loss of *TCP14* and *TCP15* function increases cuticle permeability. (A) List of cuticle biosynthesis associated genes whose expression is altered in *pTCP15::TCP15-EAR* plants. LogFC: log2 of the fold-change in expression in *pTCP15:TCP15-EAR* plants relative to wild-type (wt) plants. Details are given in Supplementary Table S2. (B) Toluidine blue staining of

3-week-old wild type (wt) and *pTCP15::TCP15-EAR* plants grown on soil. Dark blue coloration reveals a more permeable cuticle in *pTCP15::TCP15-EAR* plants. (C) Toluidine blue staining of 15-day-old plants grown in MS-agar (top) and fully expanded leaves (bottom) of wild-type (wt), *tcp14-6*, *tcp15-3*, *tcp14-4 tcp15-3* and *myb106-2* plants grown on soil. For plants grown in MS-agar, the different lines were grown in the same plate to allow uniform processing. Bars = 2 mm. (D) Chlorophyll leaching assay of whole rosettes from 3-week-old wild-type (wt), *tcp14-4 tcp15-3* and *myb106-2* plants grown on soil. The plants were placed in 80% ethanol and the release of chlorophyll was measured at the indicated times. The values are presented as the mean ± SD of six replicates for each genotype. Asterisks indicate significant differences of both mutants in comparison with the wild-type ($P < 0.05$; ANOVA). The experiment was repeated twice with similar results. (E) Total chlorophyll content in the lines of plants assayed in (D). ns, not significant ($P > 0.05$; ANOVA).

Fig. 7. TCP14 and TCP15 modulate the expression of cuticle biosynthesis genes. (A-C) Quantitative analysis of *CYP86A4*, *GPAT6*, *CUS2*, *CER2* and *LTPG2* transcript levels in developing leaves of 14-day-old *tcp14-4 tcp15-3* (A), *myb106-2* (B) and *35S::TCP15-RFP* (C) plants relative to wild-type (wt). (D) TCP15 association with the *CUS2* promoter analyzed by ChIP-qPCR. The scheme on top represents the *CUS2* genomic structure. The position of the TCP motif (TCP box) and the four regions that were analyzed by ChIP-qPCR are indicated. *PP2A* was used as a negative control. (E) and (F) Quantitative analysis of *SHN1* and *SHN2* transcript levels in young leaves of *tcp14-4 tcp15-3* mutants (E) and *35S::TCP15-RFP* plants (F) relative to wild-type (wt) plants. (G) ChIP-qPCR assay of the binding of TCP15 to the SHN1 promoter region. The scheme on top depicts the *SHN1* gene with exons shown as black boxes. The position of the two TCP motifs (TCP box) and the four regions that were analyzed by ChIP-qPCR are indicated. *PP2A* was used as a negative control. In (A-C), (E) and (F), the bars indicate the mean ± SD of three biological replicates. Asterisks indicate significant differences compared to wild-type ($P < 0.05$; Student´s *t* test). In (D) and (G), the results show the mean ± SD of three technical replicates. The experiment was repeated twice with similar results. The results of these repetitions are shown in Supplementary Fig. S5.

Fig. 8. Model for the action of TCP14 and TCP15 in the control of trichome development and cuticle biogenesis in *Arabidopsis*. TCP14 and TCP15 promote the expression of MIXTA like transcription factors to control trichome branch formation in leaves and inflorescence stems. *MYB106* is probably a direct target of TCP15. In addition, TCP14, TCP15 and MYB106 control trichome branch formation through the inhibition of DNA endoreplication by regulating the expression of cell cycle genes, like *CYCA2;3*, *CYCB1;1* and *RBR*. Cuticle formation is probably controlled by TCP14 and TCP15 at different levels: by induction of the expression of *MIXTA* and *SHN* transcription factor genes, and of *CYP86A4*, *GPAT6* and *CUS2* cuticle biosynthesis genes. *SHN* and cuticle biosynthesis genes are most likely direct and indirect targets of class I TCPs, since they are also regulated by MIXTA-like transcription factors.

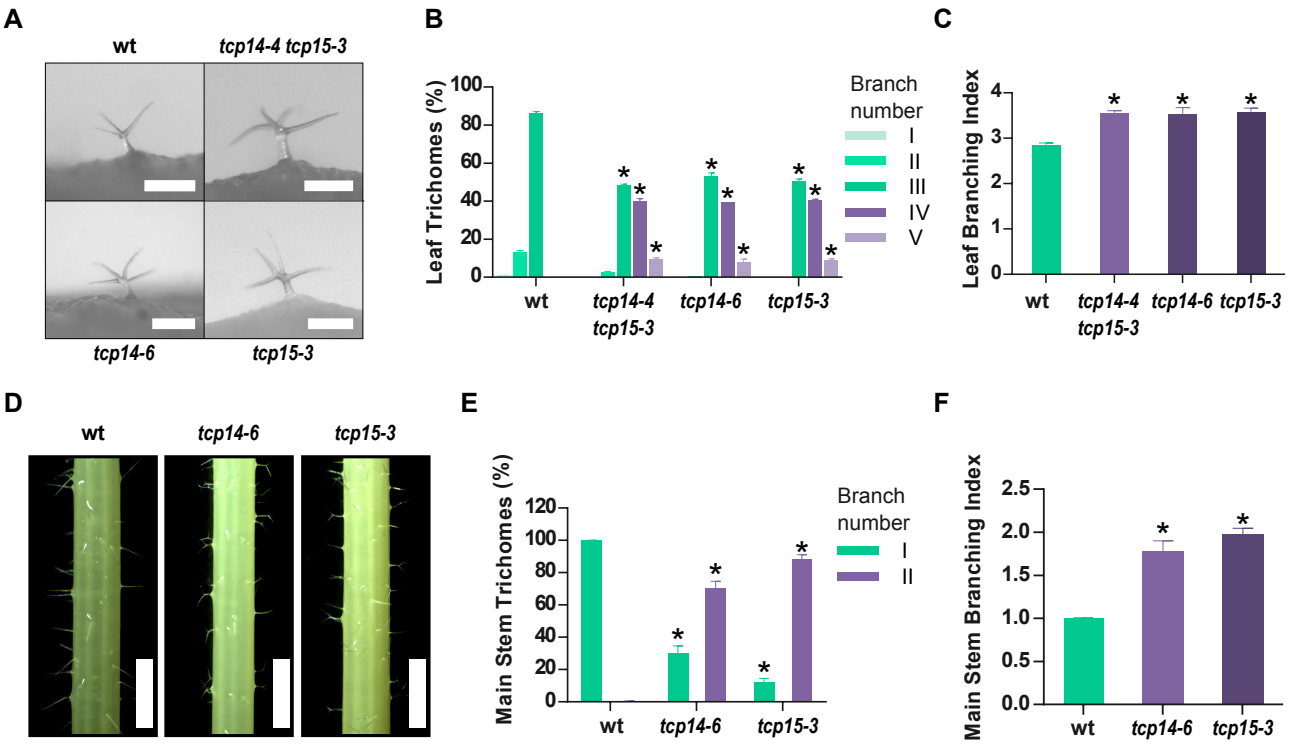

A

pTCP15::TCP15-EAR vs wt

Genes	LogFC	P-value
CML42	-1.58	1.31e-02
MYB106	-1.58	1.01e-03
MYB16	-1.23	1.13e-02

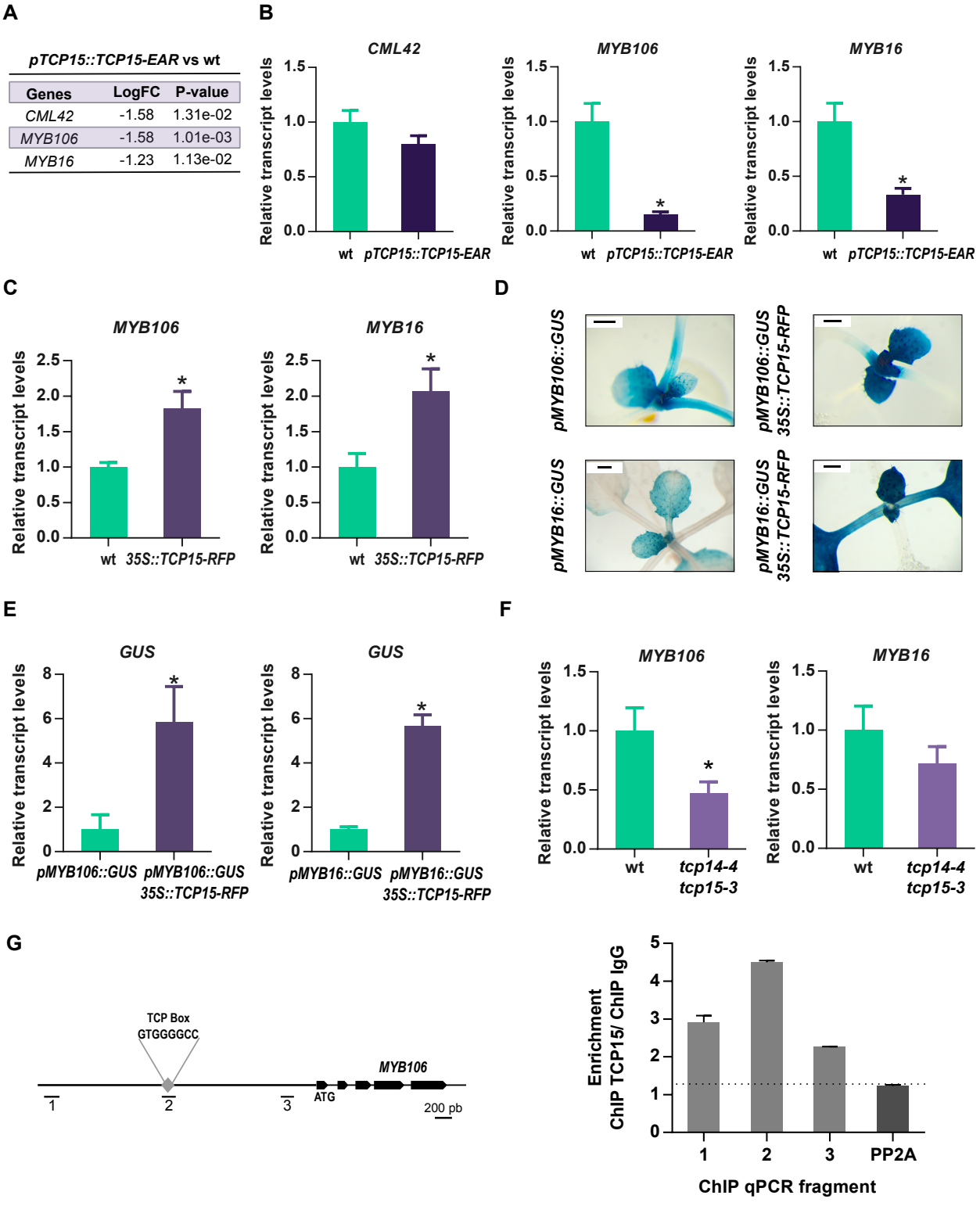

A

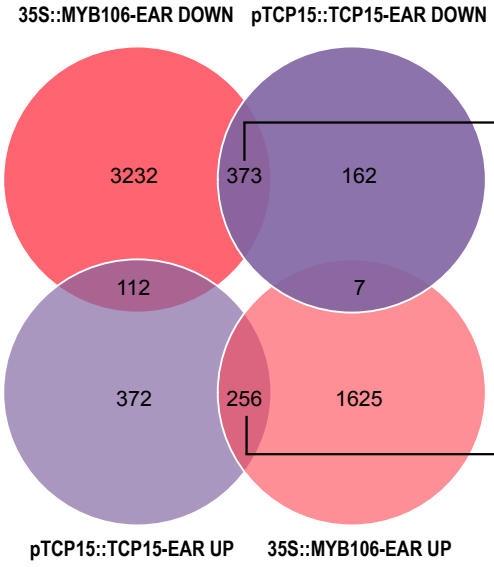

B

GO ID	Term	P-value
GO: 0045492	xylan biosynthetic process	1.4e-23
GO: 0009733	response to auxin	2.6e-12
GO: 0042546	cell wall biogenesis	1.3e-09
GO: 0009741	response to brassinosteroid	2.5e-07
GO: 0042335	cuticle development	9.7e-04
GO: 0000038	very long-chain fatty acid metabolic process	1.4e-03

GO ID	Term	P-value
GO: 0009414	response to water deprivation	3.1e-13
GO: 0009738	abscisic acid-activated signaling pathway	8.1e-09
GO: 0009611	response to wounding	8.8e-08
GO: 0010150	leaf senescence	9.1e-07
GO: 0009733	response to auxin	3.4e-05

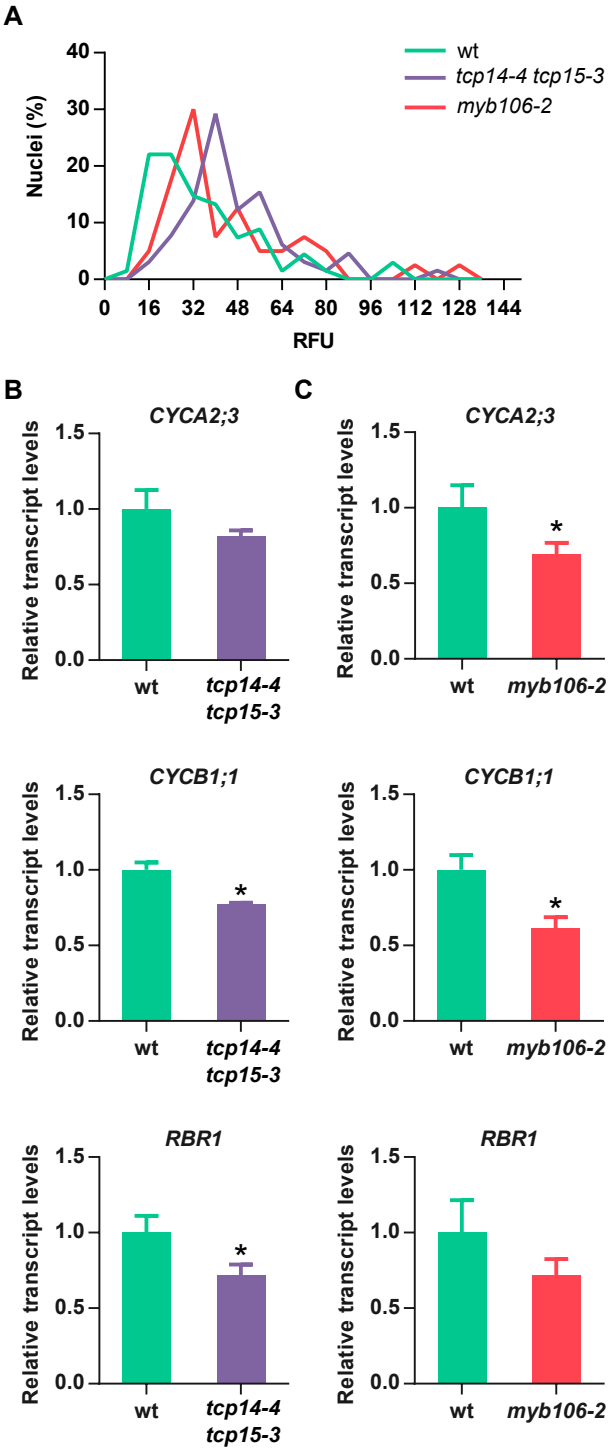

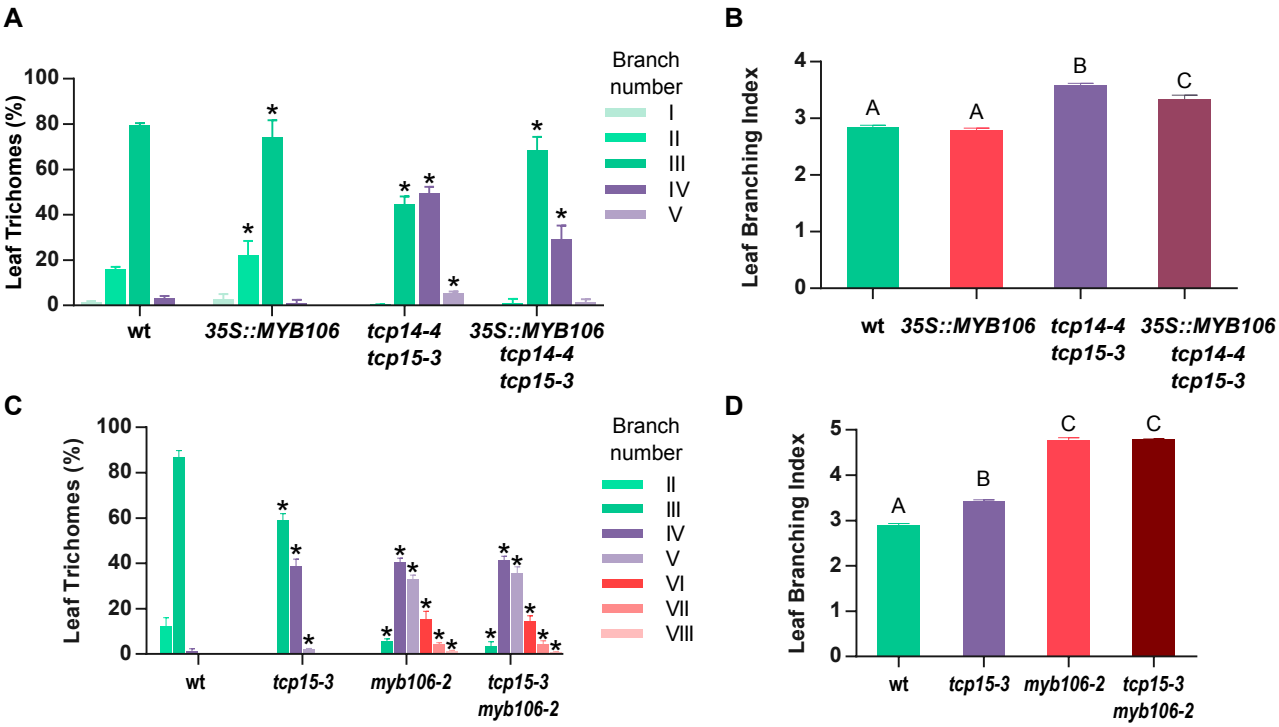

A

pTCP15::TCP15-EAR vs wt

Biosynthetic genes	LogFC	P-value
CYP86A4	-1.57	8.54e-03
CYP86A7	-1.40	1.46e-02
GPAT6	-1.44	1.71e-02
GPAT3	-1.38	1.12e-02
GPAT8	-1.16	4.70e-04
LTPG2	-1.19	1.17e-02
CER2	-1.19	1.65e-02
CUS2	-1.07	3.76e-03
Regulatory genes		
MYB106	-1.58	1.01e-03
MYB16	-1.23	1.13e-02
SHN2	-1.01	3.26e-02

B

C

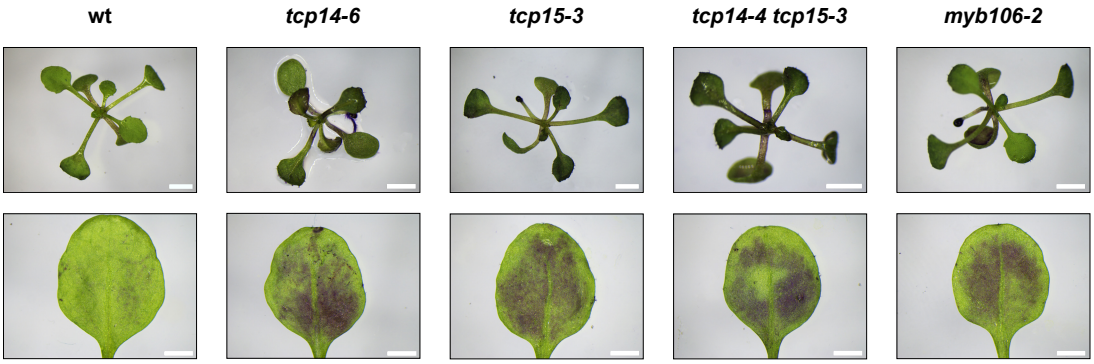

D

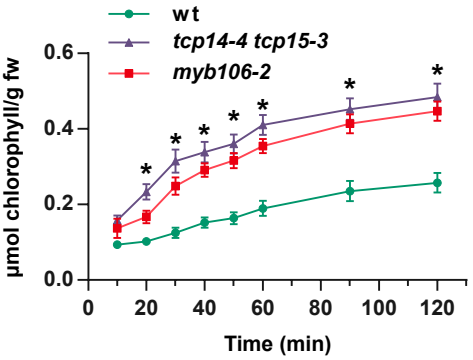

E